Middle-East Journal of Scientific Research 23 (10): 2374-2383, 2015
ISSN 1990-9233
© IDOSI Publications, 2015
DOI: 10.5829/idosi.mejsr.2015.23.10.22554

Solar Based Boost to Boost Converter Fed Nine Level Inverter System

[1]D. Jasmine and [2]M. Gopinath

[1]St. Peter's University, Chennai, India
[2]Dr. N.G.P. Institute of Technology, Coimbatore, India

Abstract: This work deals with the modelling and the simulation of PV based boost to boost converter with multilevel inverter. The output of PV system is stepped up using boost to boost converter and it is converted into AC using a multilevel inverter. The simulation results with R load, RL load and induction motor load are presented in this paper. FFT analysis is done and the THD values are compared. Boost to Boost converter is proposed to step up the voltage to the required value.

Key words: Multilevel Inverter · Boost to Boost Converter · Induction Motor Drive · THD

INTRODUCTION

THE extensive use of fossil fuels has resulted in the global problem of greenhouse emissions. Moreover, as the supplies of fossil fuels are depleted in the future, they will become increasingly expensive. Thus, solar energy is becoming more important since it produces less pollution and the cost of fossil fuel energy is rising, while the cost of solar arrays is decreas ing. In particular, small-capacity distributed power generation systems using solar energy may be widely used in residential applications in the near future [1, 2].

The power conversion interface is important to grid- connected solar power generation systems because it converts the DC power generated by a solar cell array into ac power and feeds this ac power into the utility grid.

An inverter is necessary in the power conversion interface to convert the DC power to ac power [2–4]. Since the output voltage of a solar cell array is low, a DC–DC power converter is used in a small-capacity solar power generation system to boost the output voltage, so it can match the DC bus voltage of the inverter. The power conversion efficiency of the power conversion interface is important to in- sure that there is no waste of the energy generated by the solar cell array. The active devices and passive devices in the inverter produce a power loss. The power losses due to active devices include both conduction losses and switching losses [5]. Conduction loss results from the use of active devices, while the switching loss is proportional to the voltage and the current changes for each switching and switching frequency. A filter in- doctor is used to process the switching harmonics of an inverter, so the power loss is proportional to the amount of switching harmonics.

The voltage change in each switching operation for a multi- level inverter is reduced in order to improve its power conversion efficiency [6-15] and the switching stress of the active devices. The amount of switching harmonics is also attenuated, so the power loss caused by the filter inductor is also reduced. Therefore, multilevel inverter technology has been the subject of much research over the past few years. In theory, multilevel inverters should be designed with higher voltage levels in order to improve the conversion efficiency and to reduce harmonic content and electromagnetic interference (EMI).

Conventional multilevel inverter topologies include the diode- clamped [6-10], the flying-capacitor [11-13] and the cascade H-bridge [14-18] types. Diode-clamped and flying- capacitor multilevel inverters use capacitors to develop several voltage levels. But it is difficult to regulate the voltage of these capacitors. Since it is difficult to create an asymmetric voltage technology in both the diode-clamped and the flying- capacitor topologies, the power circuit is complicated by the increase in the voltage levels that is necessary for a multilevel inverter. For a single-phase seven-level inverter, 12 power electronic switches are required in both the diode-clamped and the flying-capacitor topologies. Asymmetric voltage technology is used in the cascade H-bridge multilevel inverter to allow more levels of output

Corresponding Author: D. Jasmine, St. Peter's University, Chennai, India.

voltage [17], so the cascade H-bridge multilevel inverter is suitable for applications with increased voltage levels. Two H-bridge inverters with a DC bus voltage of multiple relationships can be connected in cascade to produce a single- phase seven-level inverter and eight power electronic switches are used. More recently, various novel topologies for seven- level inverters have been proposed. For example, a single-phase seven-level grid-connected inverter has been developed for a photovoltaic system [18]. This seven-level grid-connected inverter contains six power electronic switches. However, three DC capacitors are used to construct the three voltage levels, which results in that balancing the voltages of the capacitors is more complex. In [19], a seven-level inverter topology, configured by a level generation part and a polarity generation part, is proposed.

There, only power electronic switches of the level generation part switch in high frequency, but ten power electronic switches and three DC capacitors are used. In [20], a modular multilevel inverter with a new modulation method is applied to the photovoltaic grid-connected generator. The modular multilevel inverter is similar to the cascade H-bridge type. For this, a new modulation method is proposed to achieve dynamic capacitor voltage balance. In [21], a multilevel DC-link inverter is presented to overcome the problem of partial shading of individual photovoltaic sources that are connected in series. The DC bus of a full-bridge inverter is configured by several individual DC blocks, where each DC block is composed of a solar cell, a power electronic switch and a diode. Controlling the power electronics of the DC blocks will result in a multilevel DC-link voltage to supply a full-bridge inverter and to simultaneously overcome the problems of partial shading of individual photovoltaic sources.

This paper proposes a new solar power generation system. The proposed solar power generation system is composed of a DC/DC power converter and a nine-level inverter. The nine- level inverter is configured using a capacitor selection circuit and a full-bridge power converter, connected in cascade. The nine-level inverter contains only eight power electronic switches, which simplifies the circuit configuration.

Circuit Configuration: Fig. 1 shows the configuration of the proposed solar power generation system. The proposed solar power generation system is composed of a solar cell array, a DC–DC power converter and a new seven-level inverter. The solar cell array is connected to the DC–DC power converter and the DC–DC power converter is a boost converter that incorporates a transformer with a turn ratio of 2:1. The DC–DC power converter converts the output power of the solar cell array into two independent voltage sources with multiple relationships, which are supplied to the seven level inverter. This new nine –level inverter is Composed of a capacitor selection circuit and a full bridge power converter, connected in a cascade. The power electronic switches of capacitor selection circuit determine the discharge of the two capacitors while the two capacitors are being discharged individually or in series. Because of the multiple relationships between the voltages of the

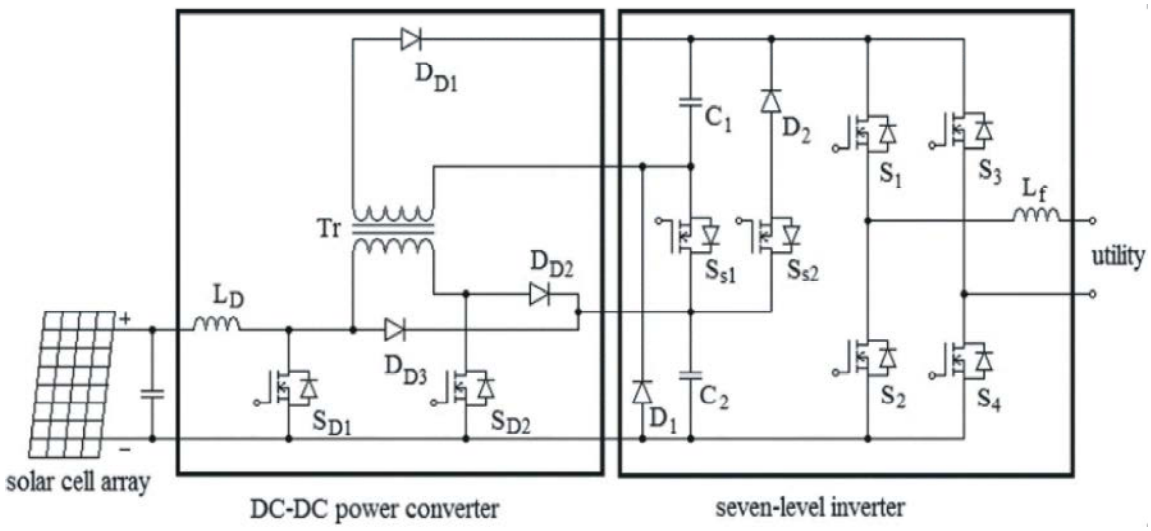

Fig. 1: Configuration of the solar power generation system

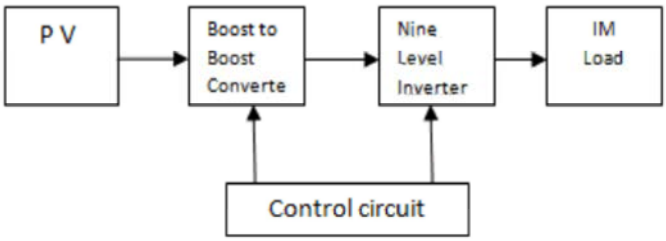

Fig. 2: Block Diagram

DC capacitors, the capacitor selection circuit outputs a three-level DC voltage. The full-bridge power converter further converts this three-level DC voltage to a seven-level AC voltage that is synchronized with the utility voltage. In this way, the proposed solar power generation system generates a sinusoidal output current that is in phase with the utility voltage and is fed into the utility, which produces a unity power factor. As can be seen, this new seven-level inverter contains only six power electronic switches, so the power circuit is simplified [21-24].

RESULTS

The simulation is done using the elements of mat lab and the results are presented here. The BBCFMLI system with the R load is shown in the Fig. 3.1. The output voltage of the solar system is 15v as shown in the Fig. 3.2. The switching pulses for the boost converter are shown in the Fig. 3.3. The output voltage of the boost converter is shown in the Fig. 3.4. The circuit of boost to boost converter is shown in the Fig. 3.5. The switching pulses for bridge 1 and bridge 2 are shown in Fig. 3.6 and 3.7

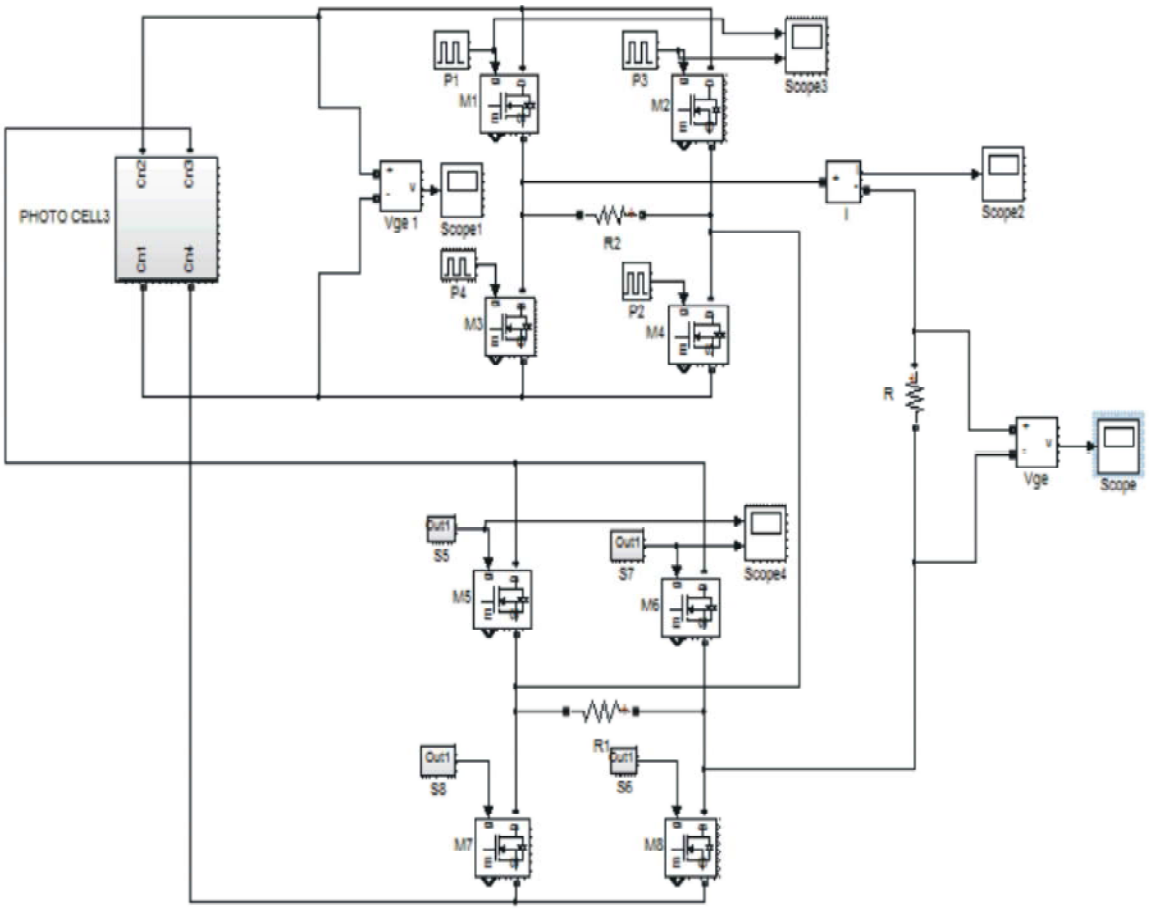

3.1 Circuit diagram of MLI with the R load

Table 1: Comparison of THD

Type of inverter	THD for R-load	THD for RL-load
Seven level	14.96%	11.42%
Nine level	7.62%	5.79%

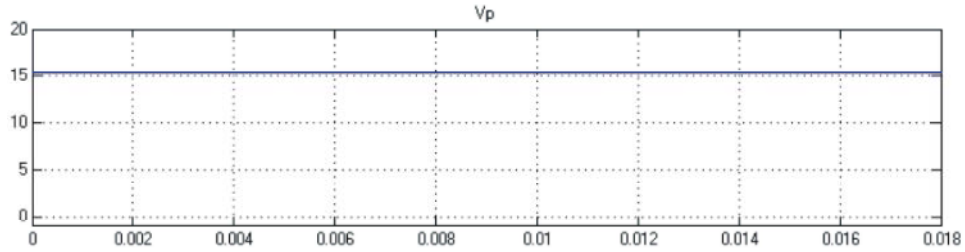

3.2: Output voltage Of the PV system

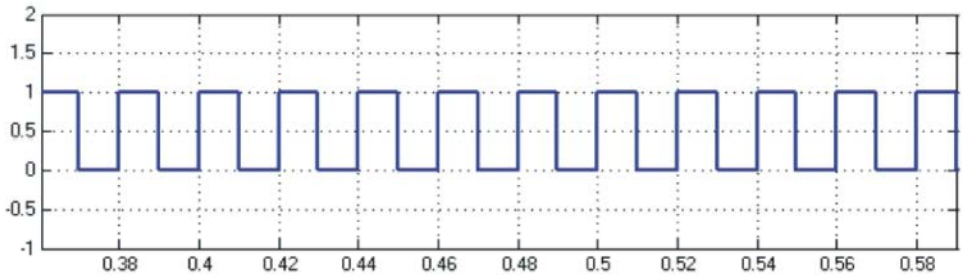

3.3: Switching pulses for the Boost Converter

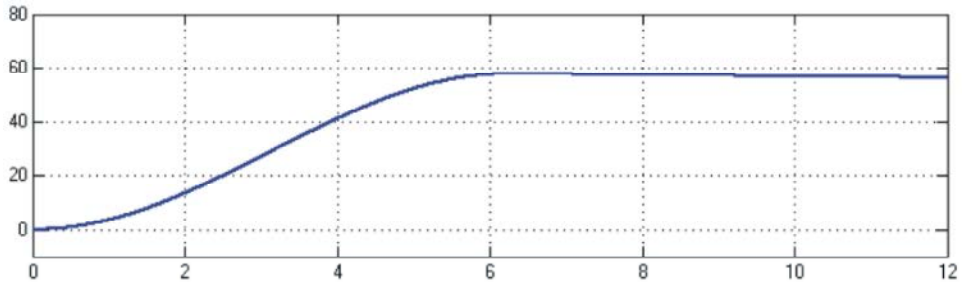

3.4: Output voltage of the Boost Converter

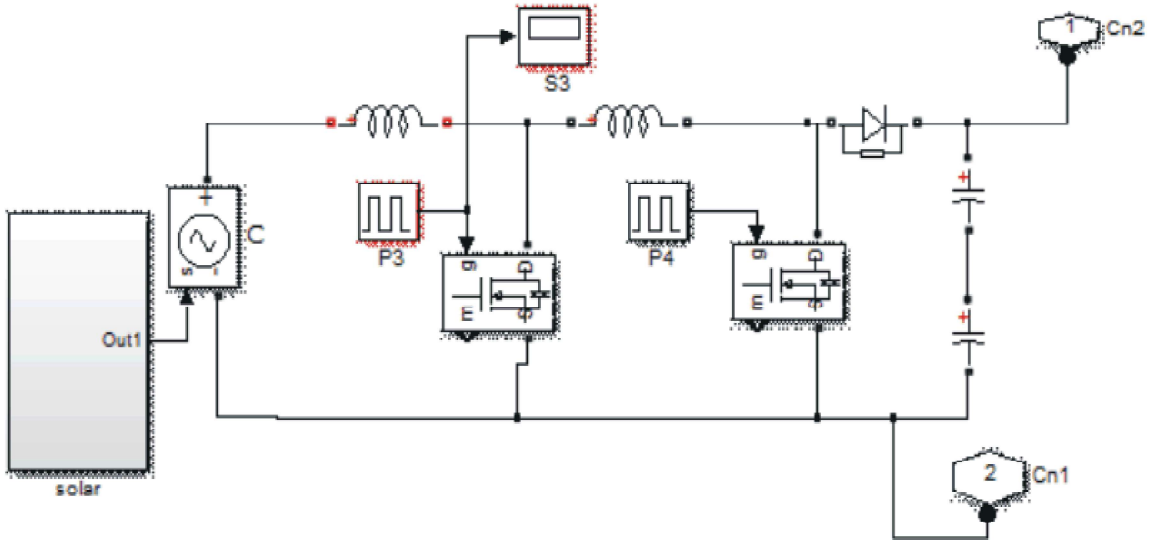

3.5: Boost to boost converter

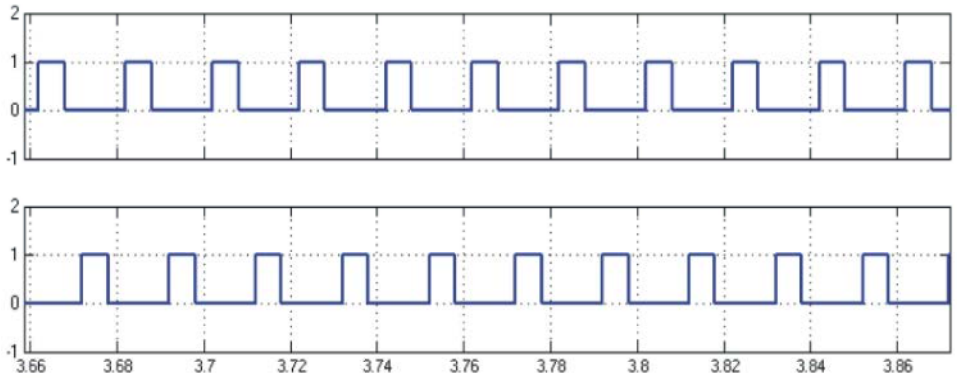

3.6: Switching pulses for the H bridge 1

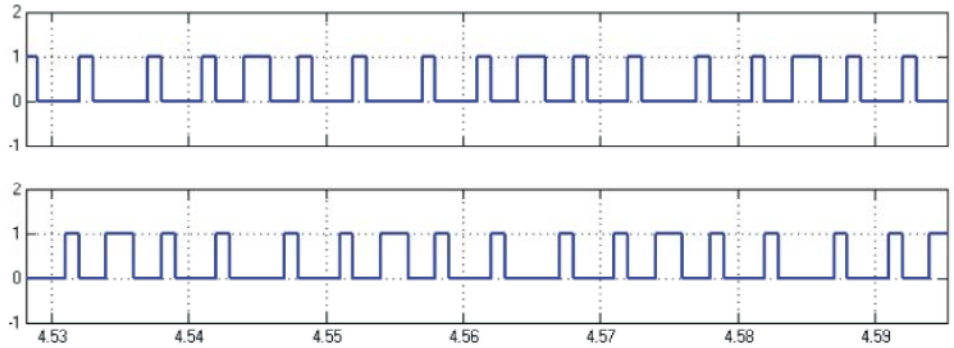

3.7: Switching pulses for the H bridge 2

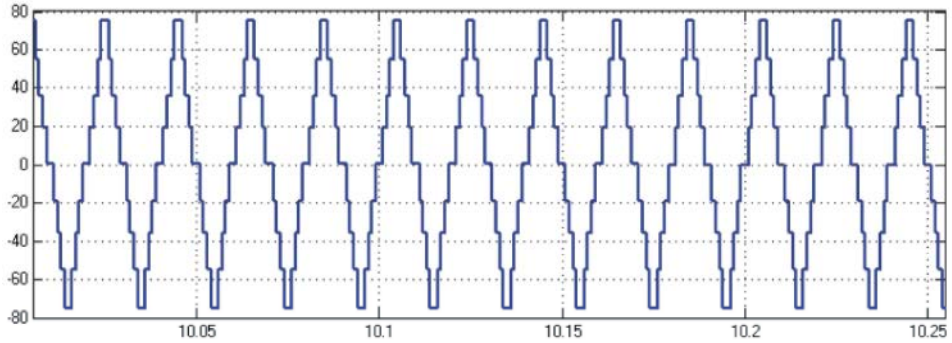

3.8: Output voltage of the MLI

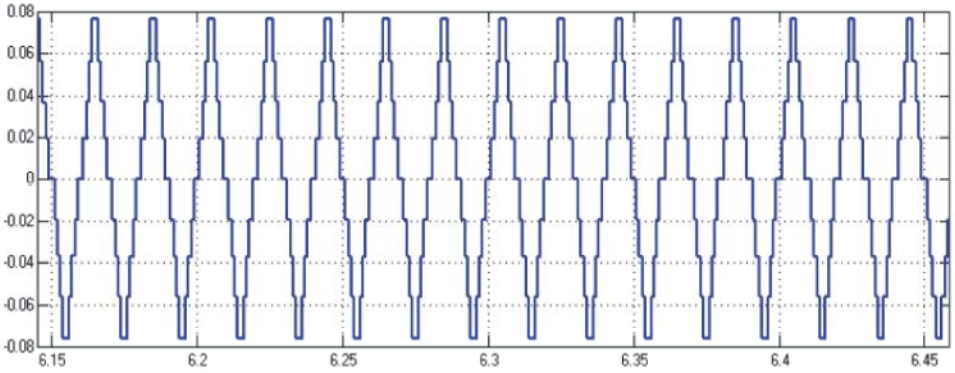

3.9: Output current of the MLI

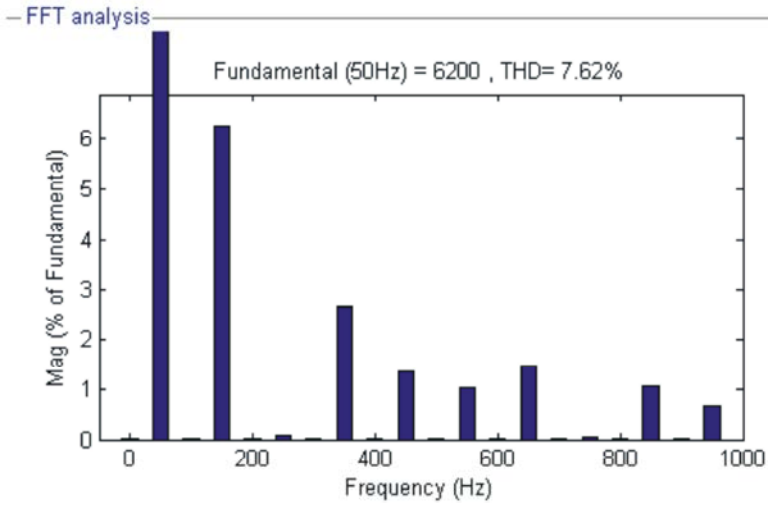

3.10: Frequency Spectrum for the Output Current

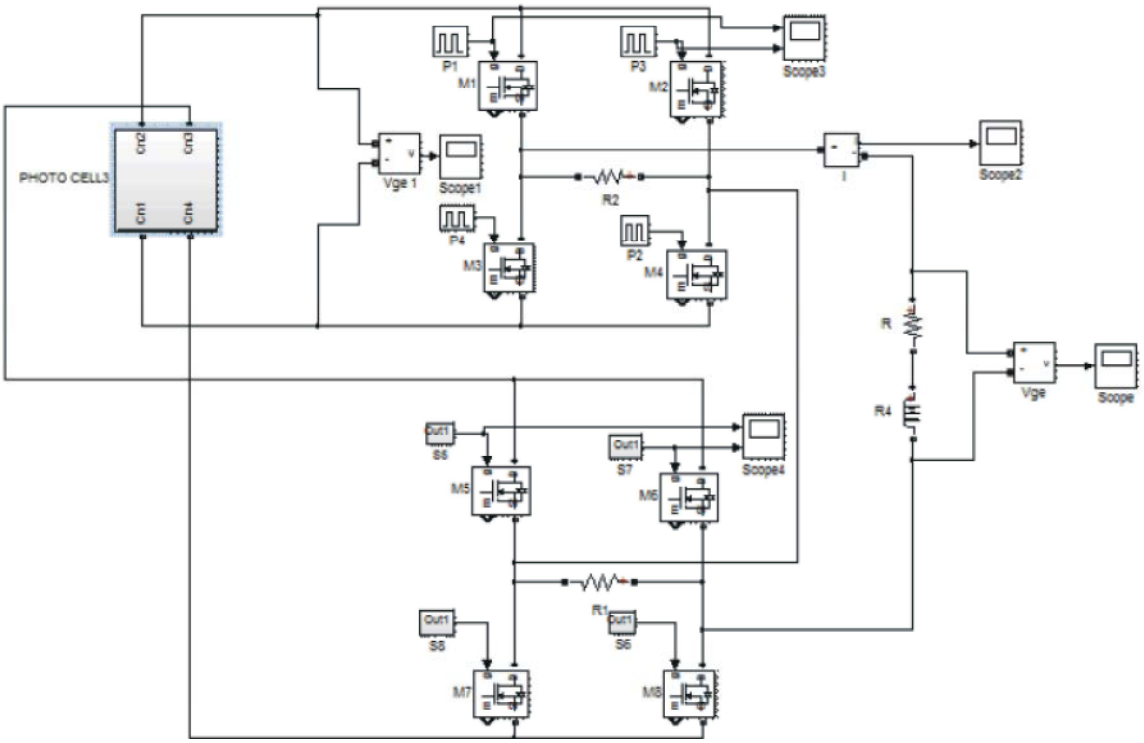

4.1: Circuit diagram of MLI with the RL load

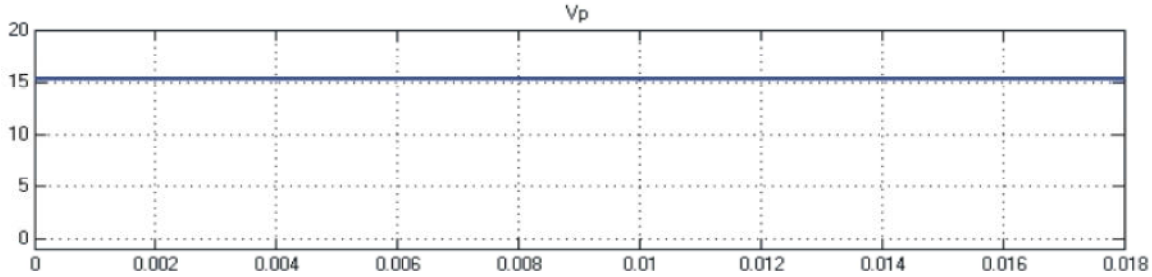

4.2: Output voltage of the PV System

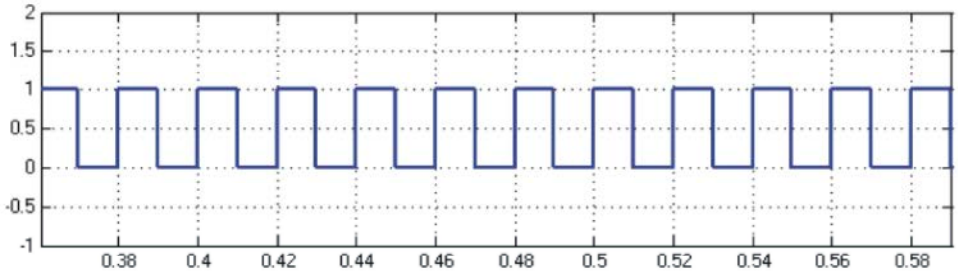

4.3: Switching pulse for the boost converter

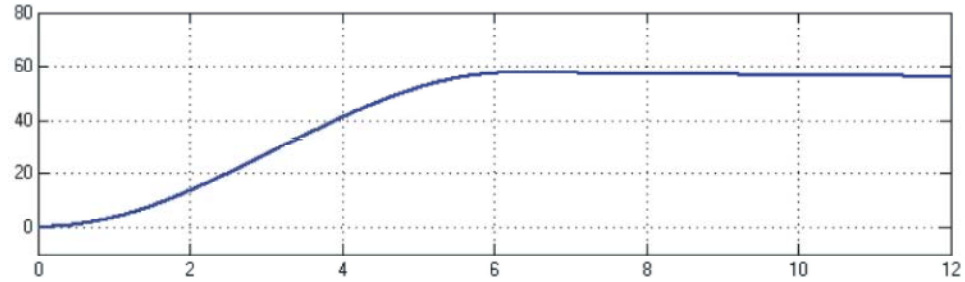

4.4: Output voltage of the Boost converter

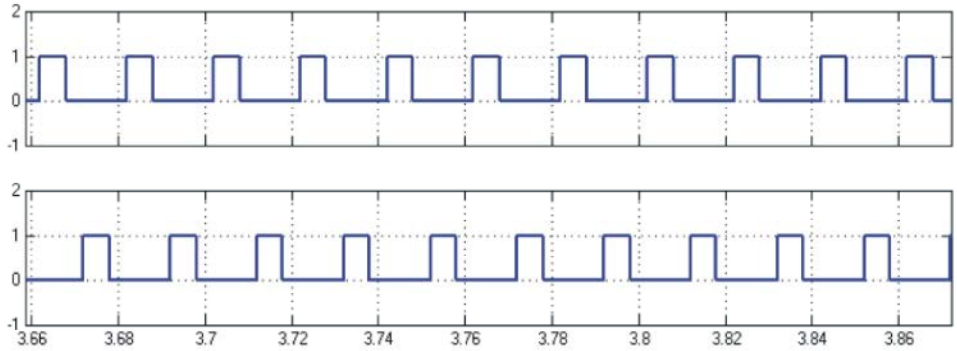

4.5: Switching pulses for the H bridge 1

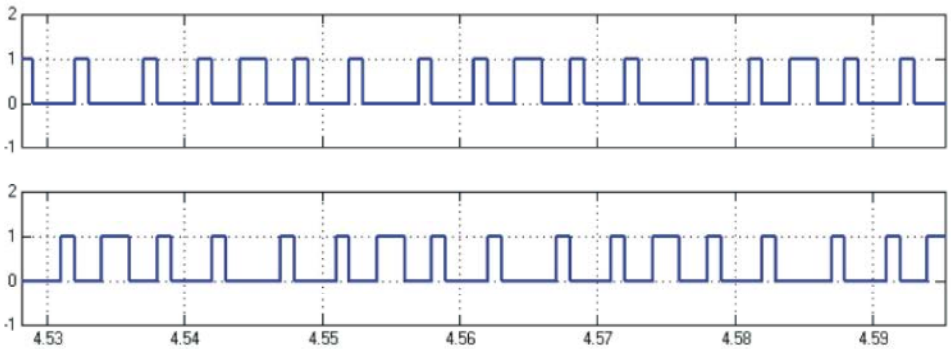

4.6: Switching pulses for the H bridge 2

respectively. Nine level output voltage and output current are shown in the Fig. 3.8 and 3.9 respectively. Frequency spectrum is shown in the Fig. 3.10. The THD is 7.62%. The BBCFMLI System with RL load is shown in Fig. 4.1. The output voltage of PV system and switching pulses for boost converter are shown in Figs. 4.2 and 4.3 respectively. The output voltage of the boost converter is shown in Fig. 4.4. Switching pulses for the bridge 1 and the bridge 2 are shown in Figs. 4.5 and 4.6 respectively. The output current and output voltage are shown in Figs. 4.7 and 4.8 respectively. The frequency spectrum is shown in the Fig. 4.9 and the THD is 5.79%.

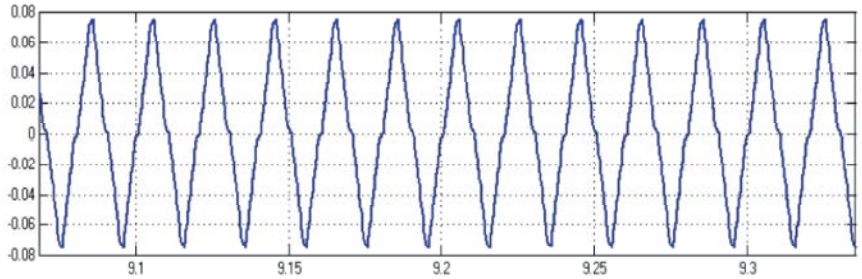

4.7: Output current of the Inverter

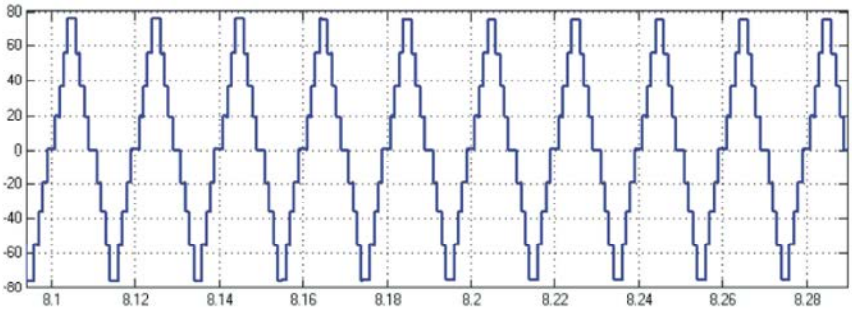

4.8: Output voltage of the Inverter

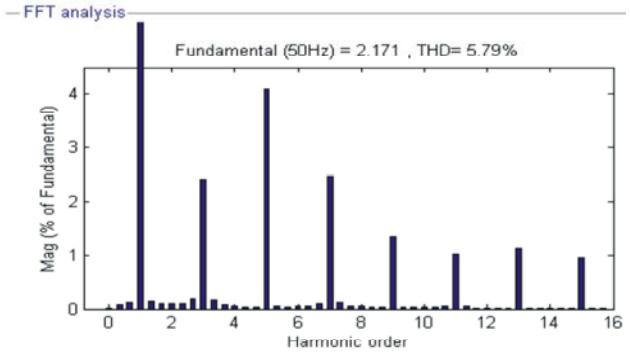

4.9: FFT Analysis for output

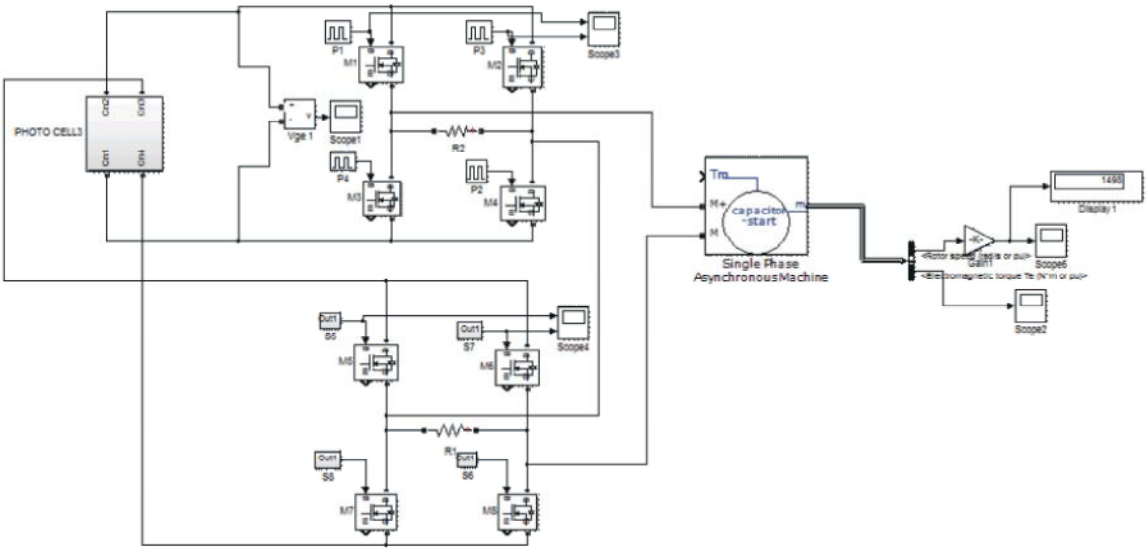

5.1: MLI System with the Induction motor Load

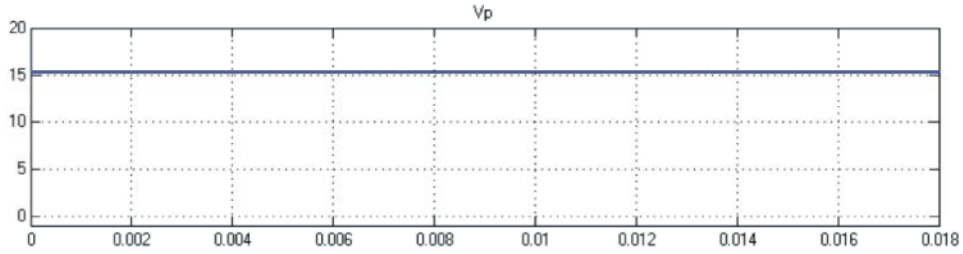

5.2: Output voltage of the PV System

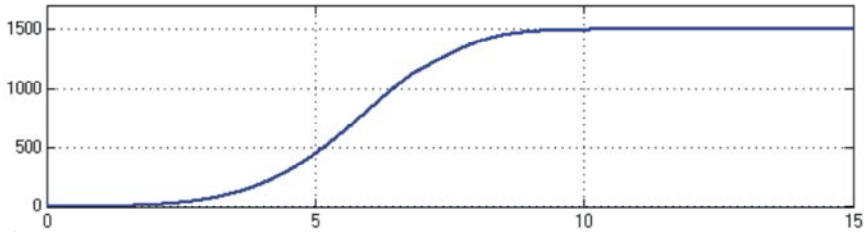

5.3: Motor speed

The MLI system with induction motor load is shown in Fig. 5.1. The output voltage of solar system is shown in the Fig. 5.2. The speed response is shown in the Fig. 5.3. The comparison of THD is given in Table 1.

CONCLUSION

The BBCFMLI System was designed, modelled and simulated successfully using Mat lab. The simulation results indicate that the THD is reduced with RL load and induction motor load. The advantages of this system are the reduction in the losses and reduction in heating of induction motor. The disadvantage of this system is that it requires two H-Bridges. This work deals with simulation of open loop control system. The closed loop system with various controllers will be investigated in future.

REFERENCES

1. Mastromauro, R.A., M. Liserre and A. Dell'Aquila, 2012. Control issues in single-stage photovoltaic systems: MPPT, current and voltage control, IEEE Trans. Ind. Informat., 8(2): 241-254.
2. Zhao, Z., M. Xu, Q. Chen, J.S. Jason Lai and Y.H. Cho, 2012. Derivation, anal- ysis and implementation of a boost-buck converter-based high-efficiency pv inverter,IEEE Trans. Power Electron., 27(3): 1304-1313.
3. Hanif, M., M. Basu and K. Gaughan, 2011. Understanding the operation of a Z-source inverter for photovoltaic application with a design example, IET Power Electron., 4(3): 278-287.
4. Shen, J.M., H.L. Jou and J.C. Wu, 2012. Novel transformer-less grid- connected power converter with negative grounding for photovoltaic gen- eration system, IEEE Trans. Power Electron., 27(4): 1818-1829.
5. Mohan, N., T.M. Undeland and W.P. Robbins, 2003. Power Electronics Con- verters, Applications and Design, Media Enhanced 3rd Ed. New York, NY, USA: Wiley.
6. Hasegawa, K. and H. Akagi, 2012. Low-modulation-index operation of a five- level diode-clamped pwm inverter with a DC-voltage-balancing circuit for a motor drive, IEEE Trans. Power Electron., 27(8): 3495-3505.
7. Pouresmaeil, E., D. Montesinos-Miracle and O. Gomis-Bellmunt, 2012. Con- trol scheme of three-level NPC inverter for integration of renewable energy resources into AC grid, IEEE Syst. J., 6(2): 242-253.
8. Srikanthan, S. and M.K. Mishra, 2010. DC capacitor voltage equalization in neutral clamped inverters for DSTATCOM application, IEEE Trans. Ind. Electron., 57(8): 2768-2775.
9. Chaves, M., E. Margato, J.F. Silva and S.F. Pinto, 2010. New approach in back-to-back m-level diodeclamped multilevel converter modelling and direct current bus voltages balancing, IET power Electron., 3(4): 578-589.
10. Barros, J.D., J.F.A. Silva and E.G.A. Jesus, 2013. Fast-predictive optimal control of NPC multilevel converters, IEEE Trans. Ind. Electron., 60(2): 619-627.

11. Sadigh, A.K., S.H. Hosseini, M. Sabahi and G.B. Gharehpetian, 2010. Double flying capacitor multicell converter based on modified phase-shifted pulsewidth modulation, IEEE Trans. Power Electron., 25(6): 1517-1526.
12. Thielemans, S., A. Ruderman, B. Reznikov and J. Melkebeek, 2012. Improved natural balancing with modified phase-shifted PWM for single-leg five- level flying-capacitor converters,IEEE Trans. Power Electron., 27(4): 1658-1667.
13. Choi, S. and M. Saeedifard, 2012. Capacitor voltage balancing of flying capacitor multilevel converters by space vector PWM, IEEE Trans. Power Delivery, 27(3): 1154-1161.
14. Maharjan, L., T. Yamagishi and H. Akagi, 2012. Active-power control of in- dividual converter cells for a battery energy storage system based on a multilevel cascade pwm converter, IEEE Trans. Power Electron., 27(3): 1099-1107.
15. She, X., A. Q. Huang, T. Zhao and G. Wang, 2012. Coupling effect reduction of a voltage-balancing controller in single-phase cascaded multilevel con- verters, IEEE Trans. Power Electron., 27(8): 3530-3543.
16. Chavarria, J., D. Biel, F. Guinjoan, C. Meza and J.J. Negroni, 2013. Energy- balance control of PV cascaded multilevel grid-connected inverters un- der level-shifted and phase-shifted PWMs, IEEE Trans. Ind. Electron., 60(1): 98-111.
17. Pereda, J. and J. Dixon, 2011. High-frequency link: A solution for using only one DC source in asymmetric cascaded multilevel inverters,IEEE Trans. Ind. Electron, 58(9): 3884-3892.
18. Rahim, N.A., K. Chaniago and J. Selvaraj, 2011. Single-phase seven-level grid-connected inverter for photovoltaic system, IEEE Trans. Ind. Electr., 58(6): 2435-2443.
19. Ounejjar, Y., K. Al-Hadded and L.A. Dessaint, A novel six-band hys- teresis control for the packed U cells seven-level converter: Experimental validation, IEEE Trans. Ind. Electron., 59(10): 3808-3816.
20. Mei, J., B. Xiao, K. Shen and L.M. Jian Yong Zheng, 2013. Modular multilevel inverter with new modulation method and its application to photovoltaic grid-connected generator, IEEE Trans. Power Electron., 28(11): 5063-5073.
21. Abdalla, I., J. Corda and L. Zhang, 2013. Multilevel DC-link inverter and control algorithm to overcome the PV partial shading, IEEE Trans. Power Electron., 28(1): 11-18.
22. Shen, J.M., H.L. Jou and J.C. Wu, 2012. Novel transformer-less grid- connected power converter with negative grounding for photovoltaic gen- eration system, IEEE Trans. Power Electron., 29(4): 1818-1829.
23. Gonzalez, R., J. Lopez, P. Sanchis and L. Marroyo, 2007. Transformerless inverter for single-phase photovoltaic systems, IEEE Trans. Power Elec- tron., 22(2): 693-697.
24. Femia, N., G. Petrone, G. Spagnuolo and M. Vitelli, 2005. Optimization of perturb and observe maximum power point tracking method, IEEE Trans. Power Electron., 20(4): 963-973.